1521-0111/88/2/357–367$25.00
MOLECULAR PHARMACOLOGY

http://dx.doi.org/10.1124/mol.115.098400
Mol Pharmacol 88:357–367, August 2015

Discovery and Characterization of Nonpeptidyl Agonists of the Tissue-Protective Erythropoietin Receptor[S]

James L. Miller, Timothy J. Church, Dmitri Leonoudakis, Karen Lariosa-Willingham, Normand L. Frigon, Connie S. Tettenborn, Jeffrey R. Spencer, and Juha Punnonen

STATegics, Inc., Menlo Park, California

Received February 13, 2015; accepted May 27, 2015

ABSTRACT

Erythropoietin (EPO) and its receptor are expressed in a wide variety of tissues, including the central nervous system. Local expression of both EPO and its receptor is upregulated upon injury or stress and plays a role in tissue homeostasis and cytoprotection. High-dose systemic administration or local injection of recombinant human EPO has demonstrated encouraging results in several models of tissue protection and organ injury, while poor tissue availability of the protein limits its efficacy. Here, we describe the discovery and characterization of the nonpeptidyl compound STS-E412 (2-[2-(4-chlorophenoxy) ethoxy]-5,7-dimethyl-[1,2,4]triazolo[1,5-*a*]pyrimidine), which selectively activates the tissue-protective EPO receptor, comprising an EPO receptor subunit (EPOR) and the common β-chain (CD131). STS-E412 triggered EPO receptor phosphorylation in human neuronal cells. STS-E412 also increased phosphorylation of EPOR, CD131, and the EPO-associated signaling molecules JAK2 and AKT in HEK293 transfectants expressing EPOR and CD131. At low nanomolar concentrations, STS-E412 provided EPO-like cytoprotective effects in primary neuronal cells and renal proximal tubular epithelial cells. The receptor selectivity of STS-E412 was confirmed by a lack of phosphorylation of the EPOR/EPOR homodimer, lack of activity in off-target selectivity screening, and lack of functional effects in erythroleukemia cell line TF-1 and $CD34^+$ progenitor cells. Permeability through artificial membranes and Caco-2 cell monolayers in vitro and penetrance across the blood-brain barrier in vivo suggest potential for central nervous system availability of the compound. To our knowledge, STS-E412 is the first nonpeptidyl, selective activator of the tissue-protective EPOR/CD131 receptor. Further evaluation of the potential of STS-E412 in central nervous system diseases and organ protection is warranted.

Introduction

Erythropoietin (EPO) is a pleiotropic cytokine primarily known as the key regulator of erythroid progenitor cell differentiation (Jacobson et al., 1957). EPO is synthesized in the renal cortex in response to erythropoietic signaling, and the distribution of EPO thus produced is generally restricted to the vasculature (Eckardt and Kurtz, 2005). EPO also exhibits broad cytoprotective and neuroprotective effects in vitro and in vivo. Biosynthesis of EPO-mediating cytoprotection occurs locally in tissues, and EPO and EPO receptor (EPOR) expression increases after injury (Juul et al., 1998; Grasso et al., 2005). EPOR can be detected in neurons, astrocytes, and microglia in the central nervous system (CNS) and in multiple peripheral organs, including the heart, kidney, liver, lung, pancreas, and skeletal muscle (Liu et al., 1997; Juul et al., 1998; David et al., 2002; Calvillo et al., 2003; Assaraf et al., 2007; Medana et al., 2009; Joshi et al., 2014).

The receptors mediating erythropoiesis and neuroprotection by EPO are distinct. A homodimeric receptor comprising two EPORs mediates erythropoiesis, and the cytoprotective effects of EPO are mediated by a heteromeric receptor composed of EPOR and the granulocyte-macrophage colony-stimulating factor (GM-CSF)/interleukin (IL)-3/IL-5 receptor common β-chain (CD131, CSF2RB) (Jubinsky et al., 1997; Brines et al., 2004; Leist et al., 2004; Chateauvieux et al., 2011). CD131 physically associates with the EPOR (Jubinsky et al., 1997; Brines et al., 2004; Bennis et al., 2012). Recombinant human EPO (rhEPO) induces phosphorylation of CD131 in UT-7 cells (Hanazono et al., 1995) and transfection of CD131 into

This work was supported by the Friedreich's Ataxia Research Alliance, the Michael J. Fox Foundation for Parkinson's Research, the National Institutes of Health National Institute of Diabetes and Digestive and Kidney Diseases [Grant 1R43-DK100140-01], and the Department of Defense ([Grant W81XWH-11-2-0009, DM090012] (U.S. Army Medical Research Acquisition Activity, 820 Chandler Street, Fort Detrick MD 21702-5014 awarding and administering acquisition office). The content is solely the responsibility of the authors and does not necessarily represent the official views of the National Institutes of Health or the U.S. government.

dx.doi.org/10.1124/mol.115.098400.

[S] This article has supplemental material available at molpharm.aspetjournals.org.

ABBREVIATIONS: BBB, blood-brain barrier; BCA, bicinchoninic acid; CEPO, carbamoylated erythropoietin; CNS, central nervous system; DMEM, Dulbecco's modified Eagle's medium; DMSO, dimethylsulfoxide; DPBS, Dulbecco's phosphate-buffered saline; ELISA, enzyme-linked immunosorbent assay; EPO, erythropoietin; EPOR, erythropoietin receptor; ER, efflux ratio; FBS, fetal bovine serum; G-CSF, granulocyte colony-stimulating factor; GM-CSF, granulocyte-macrophage colony-stimulating factor; HBSS, Hank's balanced salt solution; IL, interleukin; LDH, lactate dehydrogenase; MEM, minimum essential medium; NMDA, *N*-methyl-D-aspartate; PAMPA, parallel artificial membrane permeability assay; Papp, apparent permeability; rhEPO, recombinant human erythropoietin; RPTEC, human renal proximal tubule epithelial cells; SAR, structure-activity relationship; STS-E412, 2-[2-(4-chlorophenoxy)ethoxy]-5,7-dimethyl-[1,2,4]triazolo[1,5-*a*]pyrimidine; TPO, thrombopoietin; TPOR, thrombopoietin receptor.

EPOR-expressing Ba/F3 cells enhances the proliferative effects induced by rhEPO (Jubinsky et al., 1997). No protective effects of EPOR agonists are observed in CD131-deficient mice (Brines et al., 2004), and CD131 is crucial for rhEPO's antiapoptotic effects in endothelial cells (Su et al., 2011; Bennis et al., 2012). Like EPOR, the expression of CD131 is upregulated after tissue injury, as demonstrated by colocalization and upregulation of human EPOR and CD131 in muscle fiber sarcolemma during critical limb ischemia (Joshi et al., 2014).

rhEPO demonstrates beneficial effects in preclinical and early clinical studies in several CNS diseases such as Friedreich's ataxia, ischemic stroke, multiple sclerosis, Parkinson's disease, spinal cord injury, and traumatic brain injury (Konishi et al., 1993; Sakanaka et al., 1998; Brines et al., 2000; Erbayraktar et al., 2003; Puskovic et al., 2006; Savino et al., 2006; Mammis et al., 2009; Ehrenreich et al., 2011; Nachbauer et al., 2011; Jang et al., 2014; Punnonen et al., 2015). Achieving therapeutically meaningful levels of rhEPO in the CNS with an intact blood-brain barrier (BBB) requires direct intracranial injection or high-dose systemic administration. High-dose rhEPO, however, is associated with a risk of side effects, including thrombotic events (Drüeke et al., 2006; Singh et al., 2006), so a selective EPOR/CD131 agonist may have a therapeutic advantage over rhEPO for CNS indications.

Selective activation of the EPOR/CD131 receptor was reported using recombinant EPO variants and EPO mimetic peptides. For example, carbamoylated EPO (CEPO), desialylated derivatives of EPO, and several EPO-derived peptides signal via the tissue-protective EPOR/CD131 without any measurable erythropoietic activity (Erbayraktar et al., 2003; Brines et al., 2004, 2008; Leist et al., 2004; Coleman et al., 2006; Brines and Cerami, 2008; Ahmet et al., 2011; Chen et al., 2012). CEPO provided potent neuroprotection with efficacy comparable to high-dose rhEPO in vivo (Leist et al., 2004). However, CEPO exhibits pharmacokinetic properties similar to rhEPO (Leist et al., 2004), likely limiting the therapeutic applicability of this variant for indications where tissue-availability is critical.

Small molecules have potential advantages over proteins, particularly when tissue permeability or CNS availability is desired. Agonists of several cytokine receptors, including the receptors for granulocyte colony-stimulating factor (G-CSF) (Tian et al., 1998) and thrombopoietin (TPO) (Erickson-Miller et al., 2005; Desjardins et al., 2006; Dziewanowska et al., 2007; Kim et al., 2007; Kalota and Gewirtz, 2010; Abe et al., 2011) have been described, and the TPO receptor (TPOR) agonist eltrombopag is approved by the U.S. Food and Drug Administration for the treatment of thrombocytopenia (Kuter, 2013). The feasibility of discovering small molecule agonists of receptors for EPO was also supported by the small allosteric peptide agonists that activated the EPOR/EPOR homodimer and triggered EPO-like biologic activity (Naranda et al., 1999; Naranda et al., 2002).

We identified a series of nonpeptidyl compounds that selectively activate the tissue-protective EPOR/CD131 heteromeric receptor. The compound designated STS-E412 (2-[2-(4-chlorophenoxy)ethoxy]-5,7-dimethyl-[1,2,4]triazolo[1,5-*a*] pyrimidine) activates the EPOR/CD131 receptor at low nanomolar concentrations but does not activate the EPOR/EPOR homodimer. STS-E412 exhibits potent, EPO-like cytoprotective effects in primary human neuronal cells, rat hippocampal neurons, and human renal proximal tubule epithelial cells (RPTEC) after a range of cytotoxic challenges.

Materials and Methods

Unless otherwise indicated, we obtained the following reagents from these sources: rhEPO, NeoRecormon (Roche Pharma AG, Basel, Switzerland); recombinant human IL-3 (rhIL-3) (PeproTech, Rocky Hill, NJ); Dulbecco's modified Eagle's medium (DMEM) and minimal essential medium (MEM) cell culture media, fetal bovine serum (FBS), sodium pyruvate, L-glutamine, hygromycin B, Dulbecco's phosphate-buffered saline (DPBS), gentamycin, trypsin/EDTA, Hanks' balanced salt solution (HBSS) (all HyClone Laboratories/Thermo Fisher, Logan, UT); DNase I, leupeptin, puromycin, L-glutamate, polyethylenimine, dextrose (Sigma-Aldrich, St. Louis, MO); amphotericin B (Fungizone), B27 supplement, Neurobasal medium, Glutamax (Invitrogen/Life Technologies, Carlsbad, CA); dimethylsulfoxide (DMSO) (Fisher Scientific, Fair Lawn, NJ). STS-E412 was synthesized in our laboratory as described in the Supplemental Data.

Preparation of Human Fetal Brain Tissue. Primary human brain tissue was obtained from Advanced Bioscience Resources (Alameda, CA) as dissected 13- to 16-week-old human fetal brain tissue. The gender of the fetuses was unknown. Processing and maintenance of human cortical tissue was performed essentially according to Wogulis et al. (2005) with modifications as described herein. The initial tissue processing was performed in HBSS supplemented with 250 ng/ml amphotericin B. Brain tissue was cut into ~2-mm^3 pieces with a sterile razor blade. The tissue fragments were washed twice in amphotericin B-supplemented HBSS followed each time by centrifugation. The tissue pieces were then dispersed by trituration in amphotericin B-supplemented HBSS containing DNase I (1 mg/ml). Individual cells were separated from the tissue debris by passing the suspension through a nylon mesh cell strainer (100 μm), collected by centrifugation, and digested in 0.05% trypsin/EDTA at 37°C for 20 minutes. The digestion was terminated by adding MEM supplemented with 10% FBS and DNase I (1 mg/ml), and the cells were again dispersed by gentle trituration. The isolated cells were collected by centrifugation and washed twice in culture medium containing MEM supplemented with L-glutamine (1 mM), dextrose (1% w/v), sodium pyruvate (1 mM), B27, and gentamycin (10 μg/ml). Finally, the cells were plated in polyethylenimine-coated 24-well plates (750,000 cells per well). The medium was refreshed twice weekly, and assays were performed between 7 and 21 days in culture. The cortical cell cultures were >90% neurons, based on positive staining for neurofilament and microtubule-associated protein (Wogulis et al., 2005), and they are referred to herein as human neuronal cells.

Generation of EPOR- and EPOR/CD131-Overexpressing Cell Lines. The human embryonic kidney 293 cell line (HEK293; American Type Culture Collection, Manassas, VA) was propagated in DMEM supplemented with FBS (10%). HEK293 cells overexpressing the EPOR alone were produced by transfection with a commercial mammalian expression vector containing the human EPOR gene and a puromycin selection marker (EX-A0440-M68; Gencopoeia, Rockville MD) using the FuGENE HD transfection reagent (Promega, Madison WI) followed by selection in 5 μg/ml of puromycin. HEK293 cells overexpressing CD131 alone were produced by transfection with a commercial mammalian expression vector containing the human CSF2RB gene and a hygromycin B selection marker (EX-Z5874-M67; Gencopoeia) followed by selection in 150 μg/ml of hygromycin B. HEK293 cells overexpressing both the EPOR and CD131 were generated by transfecting the EPOR expression vector (EX-A0440-M68) into the HEK293/CD131 cell line followed by selection in puromycin and hygromycin B (5 and 150 μg/ml, respectively).

Preparation of Hippocampal Neuronal Cultures. Embryonic day-18 rat hippocampi (BrainBits, Springfield, IL) were dissociated with papain (Worthington Biochemical Corporation, Lakewood, NJ) and plated in 96-well plates at a density of 50,000 cells per well in

Neurobasal/B27 medium as follows. Brain tissue was received packaged in a proprietary preservation "Hibernate." The Hibernate medium overlaying the brain tissue was removed and replaced with 100 μg/ml of papain in DPBS (1 ml/brain); the digestion mixture was then transferred to a 30°C water bath for 30 minutes. After incubation, the digestion solution was removed and replaced with 3 ml of DMEM supplemented with 10% FBS and 2 U/ml DNase I.

With the use of a fire-polished 9-inch Pasteur pipette, the digested tissue was transferred to a 15-ml tube and triturated (5–10 cycles) to disperse the individual cells. The dispersed cells were separated from larger tissue pieces by allowing the latter to settle to the bottom of the centrifuge tube and transferring the supernatant to a new 15-ml centrifuge tube. The cells were collected by centrifugation (200*g*, 5 minutes).

The cell pellet was dispersed with a fire-polished 9-inch Pasteur pipette into 2 ml of growth medium containing Neurobasal medium, B27 supplement, and Glutamax (5 mM). The cells were plated at a density of 50,000 cells per well in 96-well multiwell plates and maintained in a humidified incubator at 37°C with 5% CO_2.

Primary Human Renal Epithelial Cells. Normal human RPTEC (Lonza/Clonetics, Basel, Switzerland) were received at passage 2 and were seeded and grown according to the manufacturer's protocol. The RPTEC were maintained in basal medium (REBM; Lonza/Clonetics) supplemented with recombinant human epidermal growth factor, recombinant human insulin, hydrocortisone, epinephrine, transferrin, triiodothyronine, gentamycin, amphotericin B, and 0.5% FBS (Lonza/Clonetics).

Signaling Assays. For assays employing HEK293 and derived cell lines, the cells were plated in 6- or 24-well plates 48 hours before the assay. For assays employing human neuronal cells, assays were performed 7 to 21 days after plating. One hour before the assay, the media were removed and replaced with fresh media. For the signaling assays measuring phosphorylation of AKT (in HEK293 and derived cells lines only), cells were detached using DPBS without Ca^{2+} or Mg^{2+}, collected by centrifugation, suspended in DMEM supplemented with 0.1% FBS, plated in 6-well tissue-culture plates, and assayed between 30–45 minutes after plating.

Compound stock solutions were prepared in DMSO at 1000× final concentration, and final dilutions were prepared immediately before the assay in cell culture medium. Compound, rhEPO, and control cultures contained identical final concentrations of DMSO (0.1% by volume). Cell plates and assay solutions were equilibrated to room temperature before the assay. The reaction was initiated by the addition of test articles (5× final concentration) and mixing by gentle trituration. After 11 minutes at room temperature, the medium overlaying the cells was removed, and the cells were washed by the addition of 1 ml of DPBS. The DPBS overlaying the cells was then removed and replaced with ice-cold lysis buffer (see Supplemental Material for the composition of the enzyme-linked immunosorbent assay [ELISA] reagents). The lysate was frozen in place, thawed, and clarified by centrifugation before analysis.

Determination of Phospho-EPOR Content in Cell Lysates. A standard sandwich ELISA was performed to assess the level of phospho-EPOR (pEPOR) according to the manufacturer's protocol (R&D Systems, Minneapolis, MN). The results were normalized to protein contents determined using the bicinchoninic acid (BCA) method (Pierce Biotechnology, Rockford, IL). See Supplemental Material, Supplemental Figs. 3–4, and Supplemental Table 1 for assay validation.

Determination of Phospho-CD131 Content in Cell Lysates. A standard sandwich ELISA was performed to assess the level of phospho-CD131 (pCD131). Briefly, total CD131 was captured with an immobilized anti–CD-131 antibody (BD Biosciences, Woburn, MA) and detected with a horseradish peroxidase–conjugated secondary antibody directed against phosphotyrosine (R&D Systems). The pCD131 content was normalized to the protein content determined using the BCA method (Pierce Biotechnology). Positive-control membrane lysates were generated using TF-1 cells that were starved of IL-3 overnight and treated with IL-3 (10 ng/ml) for 12 minutes. See Supplemental Material and Supplemental Figs. 5–7 for assay validation.

Determination of Phospho-JAK2 and Phospho-AKT Content in Cell Lysates. Commercial ELISA kits for the detection of $pY^{1007}pY^{1008}$-Janus kinase 2 (pJAK2) and pS^{473}-AKT (pAKT) were obtained from Life Technologies and Cell Signaling Technology (Beverly, MA), respectively. Both assays were performed according to the manufacturers' instructions. The pJAK2 content was quantified according to a standard provided with the kit in which 1 unit of pYpY-JAK2 is equivalent to 3.3 μg of HEL cell lysate treated with 100 μM sodium vanadate for 30 minutes. The results were normalized to protein contents determined using the BCA method (Pierce Biotechnology) and are expressed as units per 100 μg protein.

Primary Rat Cortical Neuronal Cultures. Cells were isolated from microsurgically dissected embryonic day-18 rat cortices that were obtained from Neuromics (Edina, MN), and the cultures were prepared according to the supplier's protocol.

TF-1 Cell Proliferation Assay. TF-1 cells (American Type Culture Collection) were cultured in DMEM supplemented with FBS (10%) and rhIL-3 (1 ng/ml). The cells were starved of IL-3 for 24 hours before the assay and then plated at 5000 cells per well in 96-well multiwell plates in the presence of test articles. Cell proliferation was measured 72 hours later using the CellTiter-Glo reagent (Promega) according to the manufacturer's instructions.

$CD34^+$ Cell Proliferation Assay. Frozen primary $CD34^+$ cells from human bone marrow (Stemcell Technologies, Vancouver, BC, Canada) were seeded into 96-well multiwell plates at 3000 cells/well in StemSpan serum-free expansion medium (Stemcell Technologies) containing bovine serum albumin (1%), recombinant human insulin (10 μg/ml), human transferrin (iron saturated, 200 μg/ml), 2-mercaptoethanol (20 μM), and L-glutamine (2 mM) in Iscove's modified Dulbecco's medium (Stemcell Technologies). Cell proliferation was measured after 10 days in culture using the CellTiter-Glo reagent (Promega) according to the manufacturer's instructions.

Protection of Primary Human Neuronal Cells from Staurosporine Challenge. Primary human neuronal cells were treated with STS-E412 or rhEPO for 24 hours (37°C, 5% CO_2) before initiating a staurosporine insult (500 nM, final) and incubating for an additional 24 hours. Test articles were present at the indicated concentrations for the duration of the experiment. Cytotoxicity was measured using a commercially available lactate dehydrogenase (LDH) assay kit (Clontech) according to the manufacturer's instructions.

Excitotoxicity Assay of Rat Hippocampal Cultures. After 12 days in culture, the culture medium was changed to Neurobasal medium supplemented with 0.1% bovine serum albumin but without B27 supplement, and the cultures were returned to the incubator (37°C, 5% CO_2). Test articles were added in the same medium, yielding a final concentration of 0.2% DMSO. The next day, glutamate was added to a final concentration of 100 μM, and the cell-culture plate was returned to the incubator for 24 hours. Test articles were present at the indicated concentrations for the duration of the experiment.

Cytotoxicity was measured using a colorimetric LDH assay kit (Clontech) according to the manufacturer's instructions. The total LDH activity was determined by measuring the LDH activity released by medium supplemented with 1% Triton X-100.

Hydrogen Peroxide Challenge. Twenty-four hours before the assay, RPTEC were harvested, seeded into 96-well multiwell plates, and returned to the incubator (37°C, 5% CO_2). Components contained in the RPTEC culture medium reduce hydrogen peroxide (H_2O_2); therefore, the peroxide challenge was performed in RPMI-1640 medium supplemented with 0.5% FBS. The RPTEC medium was replaced with RPMI/0.5% FBS by removing the media overlaying the cells and rinsing the tightly adhering cells with RPMI/0.5% FBS.

Fresh working stocks of H_2O_2 were prepared in HBSS. Fresh working stocks of control solutions and compounds were prepared in RPMI/0.5% FBS.

The challenge was initiated by sequential additions of 10× control or compound working stocks followed by 10× H_2O_2 working stock (150 μM final) and mixing via gentle trituration. The culture plates were returned to the incubator for 24 hours. Cytotoxicity was quantified using CellTiter-Glo and LDH release assays according to manufacturer's instructions.

Parallel Artificial Membrane Permeability Assays. Parallel artificial membrane permeability assays (PAMPAs) were performed using the precoated PAMPA Plate System (GenTest Part 353015; BD Biosciences) according to the manufacturer's protocol. DMSO stock solutions of test articles and reference compounds (dopamine, amitriptyline, propranolol, carbamazepine, sulfasalazine) were diluted in DPBS to a final concentration of 50 μM and 0.1% DMSO (v/v) and added to the donor well in a volume of 300 μl. The acceptor wells contained 50 μM Lucifer yellow in DPBS in a volume of 200 μl. Leakage of Lucifer yellow into the donor well was interpreted as a failure in the PAMPA membrane integrity. The incubation times were 2, 4, and 6 hours at room temperature.

At the conclusion of the incubation period, aliquots were removed and analyzed by reversed-phase high-performance liquid chromatography. We used an Agilent 1100 (Agilent, Santa Clara, CA) with detection at 215/254 nm, linear gradient from 0.1% trifluoroacetic acid in water (80%)/acetonitrile (20%) to 0.1% trifluoroacetic acid in water (20%)/acetonitrile (80%). Permeability (P_e), efflux ratio (ER), and mass balance were calculated according to the manufacturer's methodology (SPC-353015-G rev. 1.0). Permeability (cm/s): $P_e = \{-\ln[1 - C_A(t)/C_{eq}]\}/[A * (1/V_D + 1/V_A) * t]$, where A is the filter area (0.3 cm^2), V_D is the donor well volume (0.3 ml), V_A is the acceptor well volume (0.2 ml), t is the incubation time (seconds), $C_A(t)$ is the compound concentration in acceptor well at time t, $C_D(t)$ is the compound concentration in donor well at time t, and $C_{eq} = [C_D(t) * V_D + C_A(t) * V_A]/(V_D + V_A)$.

Caco-2 Permeability Assay. Bidirectional permeability assessment in Caco-2 cell monolayers was performed at BD Biosciences. Caco-2 cells (American Type Culture Collection) were used at passage 44 and cultured for 24 days in DMEM supplemented with 10% FBS, 5 mM HEPES, 0.4% glucose, nonessential amino acids, and 50 μg/ml gentamycin. The monolayer integrity was evaluated via pre-experimental transepithelial electrical resistance measurements and postexperimental Lucifer yellow A-to-B flux determinations for each cell monolayer. Bidirectional transport (A to B and B to A) of compounds at 10 μM (with final 0.1% DMSO v/v) was determined in duplicates at 0 and 90 minutes via liquid chromatography with tandem mass spectrometry detection in donor and acceptor wells.

Apparent permeability (Papp) was calculated according to the equation Papp (cm/s) = (Flux × V_d)/(t × A) = dQ/dt × 1/(A × C_d), where Flux is the fraction of the donated amount recovered in the receiver chamber, V_d is the volume in the donor chamber (cm^3), C_d is the initial concentration in the donor solution (in millimolar), A is the surface area of the insert filter membrane (cm^2), t is the incubation time(s), and dQ/dt is the amount of drug transported within a given time period (pmol/s).

The ER was calculated as ER = $Papp_{B\ to\ A}/Papp_{A\ to\ B}$. The mass balance was calculated as follows: Mass balance = $100 \times ((V_r \times C_r^{final}) + (V_d \times C_d^{final}))/(V_d \times C_0)$, where C_0 is the initial concentration in the donor compartment at t = 0 minute (nmol/cm^3), V_r is the volume of the receiver compartment (cm^3), V_d is the volume of the donor compartment (cm^3), C_r^{final} is the receiver concentration at the end of the incubation (nmol/cm^3), and C_d^{final} is the donor concentration at the end of the incubation (nmol/cm^3).

Off-Target Profiling Assays. Enzyme activity and radioligand binding assays against 68 pharmacologically relevant molecular targets (enzymes, receptors, ion channels) were performed at Ricerca (Concord, OH) (Part 1160393). Test articles were evaluated in duplicate at a concentration of 10 μM. All assays included a reference positive control. Significant responses were defined as ≥50% inhibition or stimulation for the biochemical assays or ≥50% inhibition of ligand binding in the radioligand binding assays. The tested molecular targets included protein serine/threonine kinase, glycogen synthase kinase-3β, adenosine A_1, adenosine A_{2A}, adenosine A_3, adrenergic α_{1A}, adrenergic α_{1B}, adrenergic α_{1D}, adrenergic α_{2A}, adrenergic β_1, adrenergic β_2, androgen (testosterone) receptor, bradykinin B_1, bradykinin B_2, calcium channel L-type (benzothiazepine), calcium channel L-type (dihydropyridine), calcium channel N-type, cannabinoid CB_1, dopamine D_1, dopamine D_{2S}, dopamine D_3, dopamine $D_{4.2}$, endothelin ET_A, endothelin ET_B, epidermal growth factor, estrogen receptor α, $GABA_A$ (flunitrazepam, central), $GABA_A$ (muscimol, central), $GABA_{B1A}$, glucocorticoid, glutamate kainate, glutamate (*N*-methyl-D-aspartate [NMDA], agonism), glutamate (NMDA, glycine), glutamate (NMDA, phencyclidine), histamine H_1, histamine H_2, histamine H_3, imidazoline I_2, IL-1, leukotriene (cysteinyl $CysLT_1$), melatonin MT_1, muscarinic M_1, muscarinic M_2, muscarinic M_3, neuropeptide Y Y_1, neuropeptide Y Y_2, nicotinic acetylcholine, nicotinic acetylcholine α1 (bungarotoxin), opiate δ1, opiate κ, opiate μ, phorbol ester, platelet activating factor, potassium channel [K_{ATP}], potassium channel human ether à go-go-related gene (hERG), prostanoid EP_4, purinergic P_{2X}, purinergic P_{2Y}, rolipram, serotonin (5-hydroxytryptamine) 5-HT_{1A}, serotonin (5-hydroxytryptamine) 5-HT_{2B}, serotonin (5-hydroxytryptamine) 5-HT_3, sigma σ_1, tachykinin NK_1, thyroid hormone, transporter, dopamine (DAT), transporter (GABA), transporter (norepinephrine NET), transporter (serotonin, 5-hydroxytryptamine).

Results

Cytoprotective EPO receptor agonist compounds were identified from a small-molecule library of putative EPO receptor agonist tool compounds (Punnonen et al., 2011). The design of the initial library was facilitated by the structure-activity relationship (SAR) information available from small molecule (Qureshi et al., 1999; Goldberg et al., 2002) and allosteric peptide (Naranda et al., 1999, 2002) agonists of the EPO receptor, and allosteric small molecule agonists of the structurally related TPOR (Erickson-Miller et al., 2005; Desjardins et al., 2006; Dziewanowska et al., 2007; Kim et al., 2007; Kalota and Gewirtz, 2010; Abe et al., 2011) as well as structural data on the receptors (Livnah et al., 1996, 1999; Carr et al., 2001). An initial hit was identified based on receptor interaction and EPO-like functional activity, and subsequent compound designs for developing an SAR for in vitro neuroprotection focused on 1,2,4-triazolo[1,5-*a*]pyrimidines. The neuroprotection SAR optimization included calculated BBB permeability [logP − (N + O) values and multiparameter optimization] (Hitchcock, 2008; Wager et al., 2010), cytoprotective activity using serum-deprived PC12 cells (Kunioku et al., 2001), aqueous solubility, in vitro metabolic stability, permeability in PAMPAs and Caco-2 assays, cytoprotection assays in primary neuronal and hematopoietic cells, and receptor activation in transfected cell lines. Compounds with EPO-like protective effects were identified, and STS-E412 was selected for more detailed characterization based on significant receptor activation, neuroprotection, and a lack of erythropoietic activity as shown below.

The structure of STS-E412 is shown as an insert in Fig. 1B, and its synthesis is described under Supplemental Material. STS-E412 has druglike physical properties (molecular weight = 318.8, cLog$P$ = 3.3, topologic polar surface area = 62 $Å^2$) and a water solubility of 0.0032 mg/ml (pH 7.0, PBS), which was determined by high-performance liquid chromatography

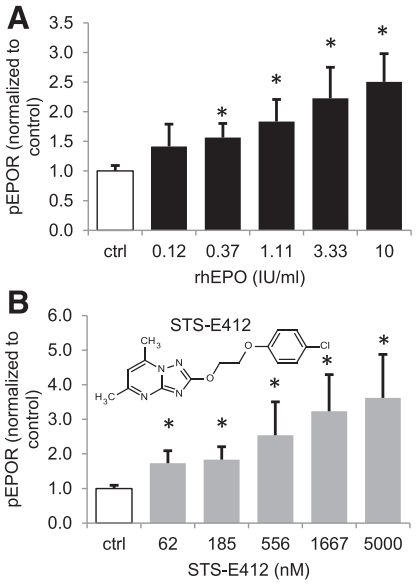

Fig. 1. RhEPO and STS-E412 increase EPOR phosphorylation in primary cultures of human cortical cells. (A) Increase in EPOR phosphorylation in response to increasing concentrations of rhEPO. (B) Increase in EPOR phosphorylation in response to increasing concentration of STS-E412. Unfilled bars represent basal phosphorylation in the absence of rhEPO or STS-E412. Solid bars (A) represent pEPOR levels measured 12 minutes after the addition of rhEPO at the indicated concentrations (IU/ml), and gray bars (B) represent phosphorylation measured 12 minutes after the addition of the indicated concentrations of STS-E412 (in nanomolar). The pEPOR levels were determined by an ELISA as described in *Materials and Methods*. The results from three independent experiments (means ± S.E.M.) using three different human cortical culture preparations are presented normalized to the respective control values. Each experiment was performed using one to three biologic replicates. Basal pEPOR levels were 0.33 ± 0.13 pg/μg (mean ± S.D., range: 0.23–0.47 pg/μg protein). *$P < 0.05$ compared with the control (basal phosphorylation) according to an unpaired Student's t test.

with UV detection analysis of the dissolved compound in a saturated solution after 90 minutes of shaking.

To evaluate EPOR activation in primary nonerythroid cells, we established cultures of primary human neuronal cells derived from human fetal cortical brain tissue. The rhEPO produced a dose-dependent increase in the amount of phosphorylated EPOR in these primary human neuronal cell cultures (Fig. 1A). Basal levels of the pEPOR averaged 0.33 ± 0.1 pg/μg protein (mean ± S.D.; range: 0.23–0.91 pg/μg). The apparent EC_{50} for rhEPO regarding EPOR phosphorylation was near 1 IU/ml (Fig. 1A), and increasing the rhEPO concentration to greater than ~10 IU/ml did not provide an additional increase in EPOR phosphorylation.

In the same primary cultures, STS-E412 also increased phosphorylation of the EPOR (Fig. 1B). The maximal effect of STS-E412 was at least comparable to or higher than that induced by rhEPO (Fig. 1B). The STS-E412–induced increase in EPOR phosphorylation was dose-dependent and significant at concentrations as low as 60 nM. STS-E412 increased pEPOR levels approximately 4-fold over background in three independent cultures of primary human neuronal cells. The increase in pEPOR in human neuronal cells produced by 10 IU/ml rhEPO ($n = 6$) was not statistically different from that produced by 5 μM STS-E412 ($n = 8$) based on Student's t test ($P = 0.479$).

To further examine signaling events induced by STS-E412, we generated HEK293 cell lines overexpressing the EPOR and CD131 (Fig. 2, A–D) or EPOR alone (Fig. 2E). In HEK293 cells overexpressing EPOR and CD131, both rhEPO and STS-E412 produced increases in EPOR and CD131 phosphorylation (Fig. 2, A and B, respectively). The basal level of pEPOR in untransfected HEK293 cells was 0.33 ± 0.3 pg/μg protein (mean ± S.D.; range: 0.01–0.86, $n = 5$), whereas cells overexpressing the EPOR and CD131 had a basal pEPOR level of 0.66 ± 0.25 pg/μg protein (mean ± S.D.; range: 0.25–0.86 pg/μg protein, $n = 4$). In these transfected cells, STS-E412 produced a dose-dependent increase in pEPOR that reached a maximum near 100 nM with a bell-shaped dose-response curve (Fig. 2A).

The magnitude of the maximal increase in pEPOR induced by STS-E412 was approximately 50% of that induced by rhEPO (Fig. 2A). Increases in pEPOR produced by 10 IU/ml rhEPO were greater than those produced by STS-E412 (tested at concentrations from 1–30 nM; $P < 0.014$) whereas increases in pEPOR produced by 10 IU/ml rhEPO versus 100 nM STS-E412 were not statistically significantly different ($P = 0.083$). Both STS-E412 and rhEPO also increased the phosphorylation of CD131 in these cells (Fig. 2B). In this case, no significant difference in the maximal response was observed between STS-E412 and rhEPO (Fig. 2B). Increases in pCD131 produced by 10 IU/ml rhEPO versus those produced by 50 nM STS-E412 were not statistically significantly different ($P = 0.21$).

Both rhEPO and STS-E412 triggered phosphorylation of JAK2 (Fig. 2C) and AKT (Fig. 2D) in HEK293 cells overexpressing the EPOR and CD131. In four independent experiments, STS-E412 increased pJAK2 by 1.52 ± 0.23-fold over basal levels with apparent EC_{50} values of approximately 1–10 nM (Fig. 2C, and unpublished data). By comparison, 10 IU/ml rhEPO increased pJAK2 by 2.2 ± 0.2-fold over basal levels (Fig. 2C). Increases in pJAK2 produced by 10 IU/ml rhEPO versus that produced by 1–3.7 nM STS-E412 were statistically different by Student's t test ($P < 0.035$) whereas increases in pJAK2 produced by 10 IU/ml rhEPO versus 11–100 nM STS-E412 were not significantly different (rhEPO versus 11 nM STS-E412, $P = 0.072$; rhEPO versus 33 nM STS-E412, $P = 0.151$; rhEPO versus 100 nM STS-E412, $P = 0.109$).

HEK293 cells and HEK293-derived cell lines contained relatively high basal levels of pAKT, and increases in pAKT above basal levels with either rhEPO or STS-E412 treatment were very small (unpublished data). To circumvent this limitation, we found that transferring cells to media containing 0.1% FBS produced a transient decrease in the level of pAKT (to approximately 30–50% of basal levels) that was persistent for approximately 1 hour (unpublished data). Under these conditions, STS-E412 also significantly increased the level of pAKT in HEK293 cells overexpressing the EPOR and CD131 (Fig. 2D). In four independent experiments, STS-E412 increased pAKT levels by 1.82 ± 0.4-fold over basal levels with apparent EC_{50} values of 1–10 nM (Fig. 2D, and unpublished data). In six independent experiments, 10 IU/ml rhEPO increased pAKT by 2.45 ± 0.91-fold over basal levels (Fig. 2D, and unpublished data). Increases in pAKT produced by 10 IU/ml rhEPO versus those produced by STS-E412 were significant at all tested concentrations ($P \leq 5.6 \times 10^{-8}$).

Using HEK293 cells overexpressing the EPOR alone, rhEPO strongly increased the phosphorylation of the EPOR (Fig. 2E), JAK2, and AKT (unpublished data) as expected. The average fold increases in the levels of pEPOR and pJAK2 produced by rhEPO were 2.7 ± 0.7-fold (mean ± S.D.; range:

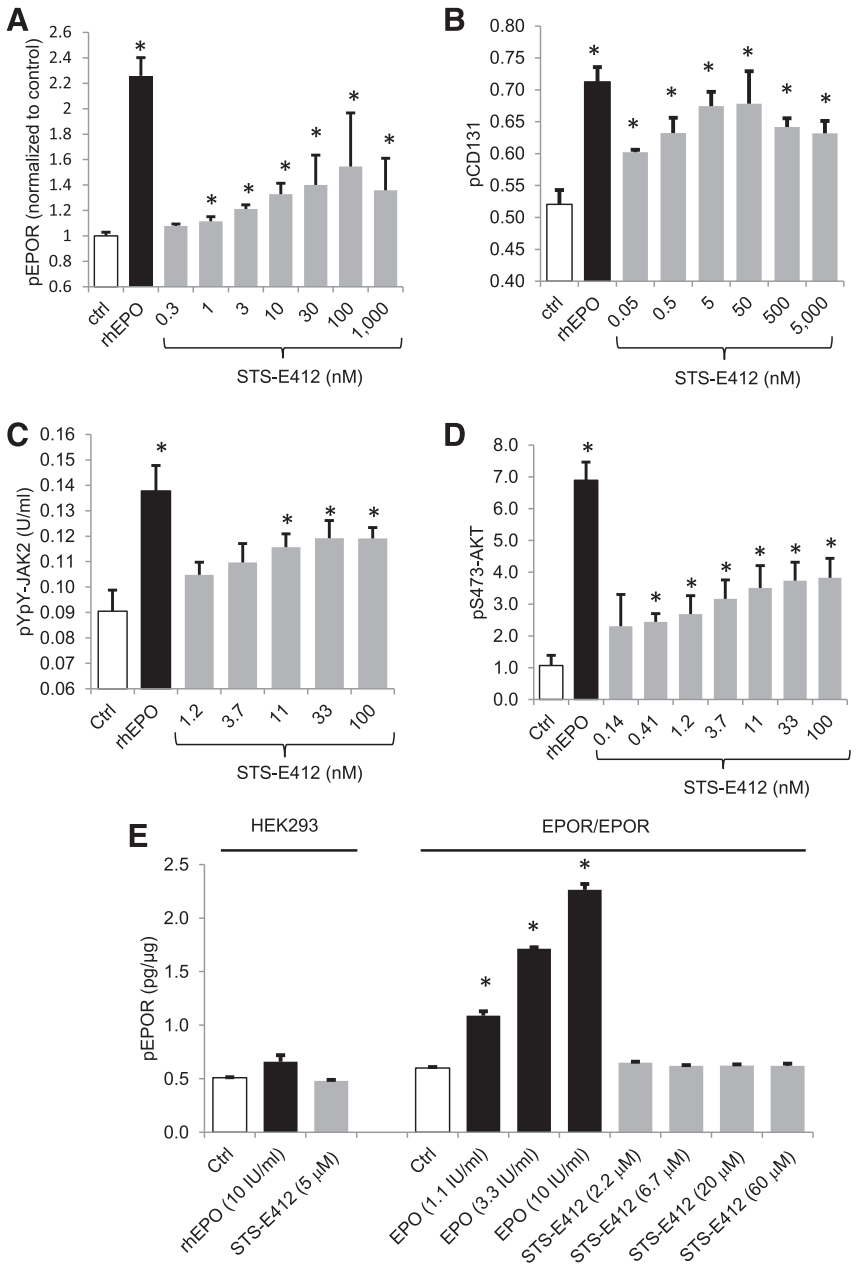

Fig. 2. STS-E412 activates the EPOR/CD131 receptor but not the EPOR/EPOR homodimer. Phosphorylation of the EPOR, CD131, and the signaling molecules JAK2 and AKT were studied in HEK293 cells coexpressing the EPOR and CD131 (A–D) or in HEK293 cells expressing only the EPOR (E). In all the figures, the unfilled bars represent basal phosphorylation in the absence of rhEPO or STS-E412, solid bars represent phosphorylation levels measured 12 minutes after the addition of rhEPO (10 IU/ml), and gray bars represent phosphorylation measured 12 minutes after the addition of the indicated concentrations of STS-E412 (in nanomolar). Phosphoprotein levels were determined by an ELISA as described in *Materials and Methods*. (A) Increase in pEPOR induced by rhEPO and STS-E412. The data represent increases in pEPOR (mean ± S.E.M.) from five independent experiments; each experiment included three to six replicate measurements. Basal pEPOR levels were 0.66 ± 0.25 pg/µg (mean ± S.D.). (B) Increase in pCD131 induced by rhEPO and STS-E412. The data are representative of three independent experiments (mean ± S.E.M.; each experiment included two to three biologic replicates). (C) Increase in $pY^{1007}pY^{1008}$-JAK2 induced by rhEPO and STS-E412. The data are representative of two independent experiments, each performed in two or eight biologic replicates. (D) Increase in pS^{473}-AKT induced by rhEPO and STS-E412. The data are representative of three independent experiments each performed in two to eight biologic replicates (mean ± S.E.M.). (E) STS-E412, in contrast to rhEPO, does not increase EPOR phosphorylation in HEK293 cells or HEK293 cells overexpressing EPOR alone. The data represent averaged increases in pEPOR from triplicate measurements under control conditions (unfilled bars), in the presence of rhEPO (solid bars), or in the presence of STS-E412 (gray bars). The cells were exposed to rhEPO or STS-E412 at the indicated concentrations for 12 minutes, and the reaction was quenched by the addition of a lysis buffer. Similar results were obtained in five independent experiments and at concentrations of STS-E412 ranging from 1 to 60,000 nM. $^*P < 0.05$ compared with the control (Ctrl) according to Student's *t* test.

1.9–3.6, $n = 5$) and 7.9 ± 4.3 (mean ± S.E.M.; range: 2.7–20.8, $n = 4$), respectively. The fold increases in pAKT levels (1.45-fold over the basal level) in the presence of 0.1% FBS and in response to rhEPO were smaller than the increases in pEPOR and pJAK2. In untransfected HEK293 cells, rhEPO produced a small, statistically insignificant increase in pEPOR ($P = 0.062$, triplicate measurements; Fig. 2E), whereas pEPOR levels in the presence of STS-E412 were indistinguishable from those in the controls. In EPOR-overexpressing HEK293 cells, rhEPO produced an increase in pEPOR in a dose-dependent manner. In contrast, STS-E412 at concentrations ranging from 1 nM to 60 µM did not increase pEPOR levels in the HEK293 cells overexpressing the EPOR alone (Fig. 2E, and unpublished data). Increases in pEPOR produced by 10 IU/ml rhEPO versus those produced by STS-E412 (tested at concentrations from 2–60 µM) were significant at all tested concentrations ($P \leq 0.00011$). Consistent with our finding in HEK293 cells, STS-E412 did not produce increases in pEPOR in the erythroid cell line TF-1 over a similar concentration range, whereas 10 IU/ml rhEPO resulted in increases in pEPOR of approximately 2-fold (1.94 ± 0.16-fold, mean ± S.D.; range: 1.83–2.12, $n = 3$; unpublished data).

Proliferation assays with the erythroleukemia cell line TF-1 (Fig. 3, A and B) and primary human bone marrow-derived $CD34^+$ cells (Fig. 3, C and D) support the view that STS-E412 does not stimulate the erythropoietic EPOR/EPOR homodimer. RhEPO induced dose-dependent increases in both TF-1 and $CD34^+$ cell numbers (Fig. 3, A and C, respectively). In contrast, STS-E412 at concentrations up to 1000 nM had no effect on TF-1 or $CD34^+$ cell proliferation (Fig. 3, B and D, respectively). At concentrations above 1000 nM, STS-E412 decreased the proliferation of TF-1 cells (Fig. 3B), while the proliferation of $CD34^+$ cells was increased (Fig. 3D). Student's *t* test comparing TF-1 proliferation in the presence of 10 IU/ml

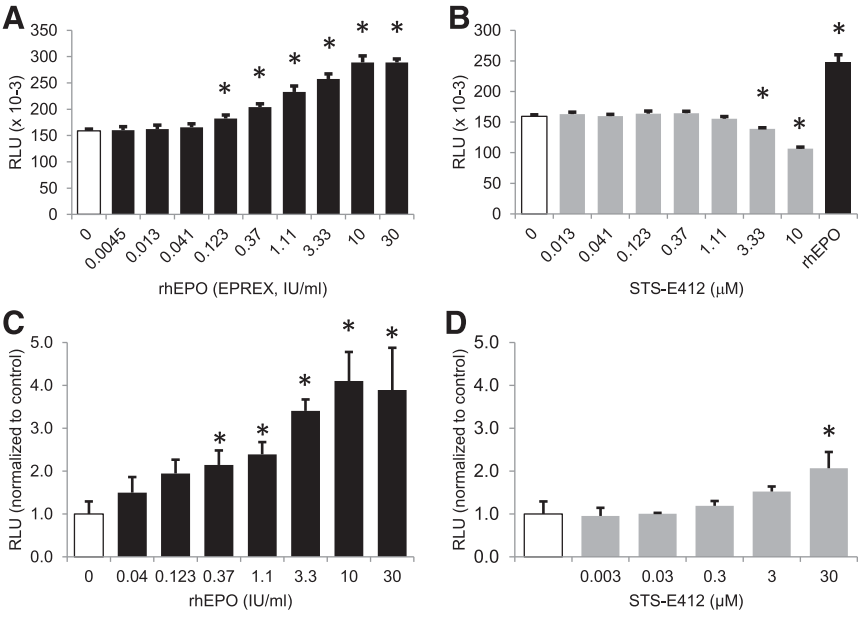

Fig. 3. Effects of rhEPO and STS-E412 on proliferation of TF-1 and primary human CD34$^+$ cells. TF-1 cells (A and B) were starved of IL-3 for 24 hours before the experiment. Then rhEPO (A) or STS-E412 (B) were added to the cells at the indicated concentrations, and the cells were returned to a humidified 37°C CO_2 incubator for 72 hours. Proliferation was measured by increases in ATP using a luminescence detection assay (CellTiter-Glo; Promega). The data represent the results of six (STS-E412) or eight (control, rhEPO) replicate cultures (mean ± S.E.M.). The results are representative of three independent experiments. (C and D) Effects of (C) rhEPO and (D) STS-E412 on the proliferation of primary human CD34$^+$ cells. We added rhEPO or STS-E412 to yield the indicated concentrations, and the cells were returned to a humidified 37°C incubator with 5% CO_2 for 10 days. Proliferation was measured by increases in ATP using a luminescence detection assay (CellTiter-Glo; Promega). The data represent the mean ± S.E.M. of two independent experiments, each performed in triplicate and normalized to the respective control values. Controls are represented by unfilled bars; rhEPO is represented by solid bars, and STS-E412 is represented by gray bars. RLU, relative luminescence units. *$P < 0.05$ compared with the control according to Student's t test.

rhEPO versus STS-E412 (Fig. 3B) indicated these differences were statistically significant ($P < 8.03 \times 10^{-5}$). In contrast, Student's t tests comparing CD34$^+$ cell proliferation in the presence of 10 IU/ml rhEPO versus 30 μM STS-E412 were not statistically significant ($P = 0.11$); the differences between 10 IU/ml rhEPO and STS-E412 at 3 μM and lower concentrations were statistically significant ($P < 0.024$).

STS-E412 protected primary human neuronal cells from a staurosporine challenge (Fig. 4A), protected primary rat hippocampal neurons from an excitotoxic glutamate challenge (Fig. 4B), and protected primary human RPTEC from a H_2O_2 challenge (Fig. 5, A and B). All the protection assays followed a paradigm consisting of a 24-hour treatment with the test articles followed by a 24-hour challenge, and rhEPO was included in the experiments for comparison.

In human neuronal cells (Fig. 4A), the basal extracellular LDH was 19.3 ± 1.7% of the total LDH (mean ± S.D.). Staurosporine treatment alone (500 nM) increased the extracellular LDH to 36.8 ± 7.2% of the total LDH (mean ± S.D., 1.9-fold increase). Pretreatment with rhEPO attenuated the staurosporine-dependent increase in the extracellular LDH by approximately 40% (to 29.9 ± 2.9% of the total LDH). STS-E412 also protected the human neuronal cells from a staurosporine insult in a dose-dependent manner with an apparent EC_{50} value in the 1–10 nM range (Fig. 4A). STS-E412 attenuated the increase in extracellular LDH by approximately 50% at concentrations above 10 nM (e.g., to 27.3 ± 1.6% of the total LDH in the presence of 1000 nM STS-E412). Based on Student's t tests, the differences in protection from staurosporine insult of human neuronal cells produced by 10 IU/ml rhEPO versus those produced by STS-E412 at concentrations ≥1 nM were not statistically significant (rhEPO versus STS-E412 at 1 nM, $P = 0.097$; rhEPO versus STS-E412 10 nM, $P = 0.697$; rhEPO versus STS-E412 at 100 nM, $P = 0.361$; rhEPO versus STS-E412 at 1000 nM, $P = 0.547$).

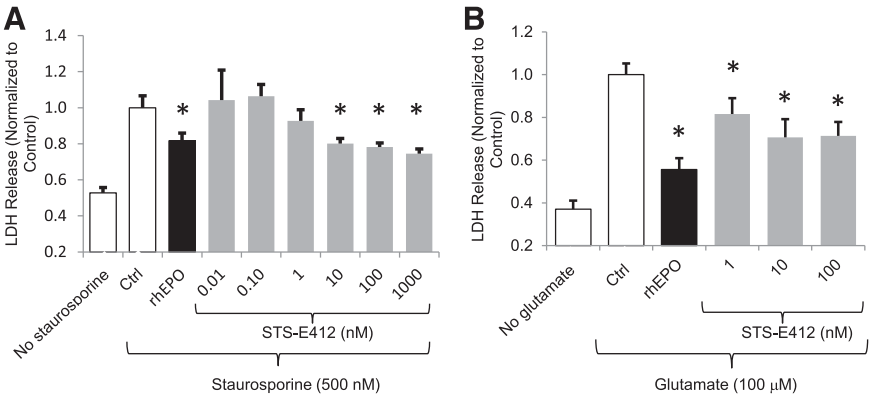

Fig. 4. STS-E412 protects primary human and rat neuronal cells from cytotoxic insults. (A) Primary human cortical cells were pretreated with STS-E412 at the indicated concentrations or rhEPO (10 IU/ml) for 24 hours before a staurosporine insult (500 nM). After culturing the cells for an additional 24 hours, the supernatants were harvested, and the LDH levels were measured as described in the *Materials and Methods* section. The data represent the mean ± S.E.M. of six (rhEPO, STS-E412) or nine (control [Ctrl], staurosporine alone) replicates. (B) Primary rat hippocampal cells were pretreated with STS-E412 at the indicated concentrations or rhEPO (10 IU/ml) for 24 hours before a glutamate insult (100 μM). The cells were then cultured for an additional 24 hours. The supernatants were harvested, and the LDH levels were measured as above. *$P < 0.05$ compared with the control according to Student's t test.

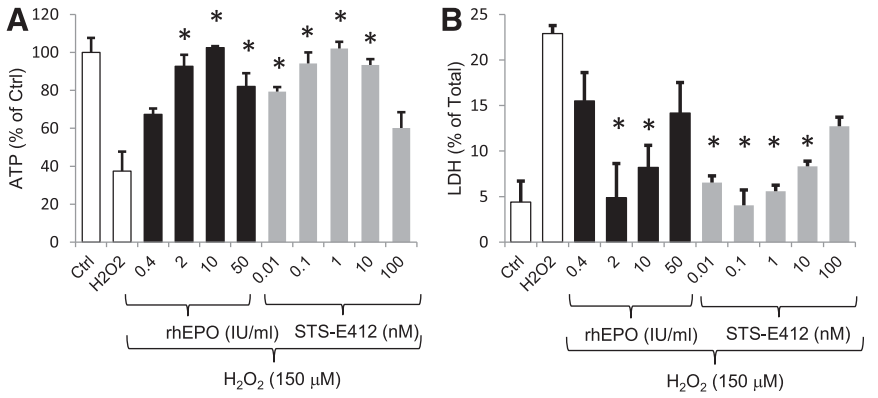

Fig. 5. STS-E412 protects primary human RPTEC from H_2O_2-mediated cytotoxicity. RPTEC were pretreated with STS-E412 or rhEPO at the indicated concentrations for 24 hours before H_2O_2 insult (150 μM). The cells were then treated with H_2O_2 and returned to a 37°C 5% CO_2 incubator for another 24 hours. CellTiter Glo (A) and LDH assays (B) were then performed. Unfilled bars indicate control values (insult only); solid bars represent measured values in the presence of rhEPO (10 IU/ml), and gray bars indicate measured values in the presence of STS-E412 at the indicated concentrations. LDH and ATP levels were measured as described in *Materials and Methods*. The data represent the mean ± S.E.M. of six (control [Ctrl], H_2O_2 alone) or three (rhEPO, STS-E412) replicates. *$P < 0.05$ compared with the control according to Student's t test.

In primary rat hippocampal neuronal cultures, pretreatment with rhEPO attenuated the glutamate-dependent increase in extracellular LDH by approximately 70%. Similarly, STS-E412 protected primary rat hippocampal neurons from glutamate challenge with a maximal protection at concentrations above 10 nM (Fig. 4B). Concentrations of STS-E412 above 10 nM attenuated the increase in extracellular LDH by up to 46 ± 16%. Based on Student's t tests, 10 IU/ml rhEPO produced significantly greater protection from glutamate insult in rat hippocampal neurons than STS-E412 (rhEPO versus STS-E412 at 1 nM, $P = 0.0071$; rhEPO versus STS-E412 10 nM, $P = 0.0128$; rhEPO versus STS-E412 at 100 nM, $P = 0.0133$).

In primary cultures of human RPTEC, pretreatment with rhEPO attenuated the H_2O_2-dependent decrease in intracellular ATP in a dose-dependent manner with complete or near-complete protection in the 1–10 IU/ml concentration range (102 ± 0.75% of control at 10 IU/ml rhEPO; Fig. 5A). This protection was also reflected in a decrease in the level of extracellular LDH at similar rhEPO concentrations; rhEPO attenuated the increase in extracellular LDH by greater than 79% (97.5 ± 25% for 2 IU/ml rhEPO and 79.4 ± 0.1% for 10 IU/ml rhEPO). Pretreatment with STS-E412 also attenuated the H_2O_2-dependent decrease in intracellular ATP in a dose-dependent manner with nearly complete protection at low nanomolar concentrations and complete protection at concentrations near 1 nM (103.3 ± 3.8% at 1 nM STS-E412; Fig. 5A). This protection was also reflected in a decrease in extracellular LDH at similar STS-E412 concentrations, and complete protection was observed at 0.1 nM STS-E412 (102 ± 13% compared with the unchallenged control; Fig. 5B).

Based on Student's t test, 10 IU/ml rhEPO did not produce significantly more protection form H_2O_2 challenge than the optimal concentration of STS-E412 (LDH read-out: rhEPO versus 0.1 nM STS-E412, $P = 0.303$; Cell Titer Glo readout: rhEPO versus 1 nM STS-E412, $P = 0.933$). Protection from H_2O_2 challenge was reduced at the highest concentrations of rhEPO and STS-E412 (Fig. 5, A and B).

A preliminary assessment of the suitability of STS-E412 for in vivo studies was performed using permeability and off-target activity assays. STS-E412 demonstrated high in vitro permeability in a PAMPA with a P_e value of 15×10^{-6} cm/s. The bidirectional transport of STS-E412 at 10 μM across a Caco-2 cell monolayer was determined via liquid chromatography with tandem mass spectrometry detection. STS-E412 demonstrated high transcellular permeability in both directions, with Papp values $>17 \times 10^{-6}$ cm/s. The calculated ER was <1.0, suggesting that the compound is not a substrate for P-glycoprotein, a BBB efflux transporter.

Importantly, permeability of STS-E412 across the BBB was observed in vivo. Thirty minutes after 10 mg/kg intraperitoneal dose of STS-E412 in Sprague-Dawley rats ($n = 3$), plasma and brain concentrations of the compound were 4073 ± 121 ng/ml and 1589 ± 25 ng/ml, respectively (compound calculations for brain homogenate are based on a density of 1 ml/g of tissue; see Supplemental Material for experimental details). The calculated brain/plasma concentration ratio was 0.39. Next, potential off-target effects were evaluated in an enzyme- and radioligand-binding panel of 68 molecular targets. The assay package was designed for prioritizing drug candidates using a broad selection of targets to detect the drug's potential for adverse events and included several CNS targets to evaluate the potential for drug dependence (the complete list of targets is presented in *Materials and Methods*). Significant responses were defined as >50% inhibition or stimulation at 10 μM. All the assay values for STS-E412 were <50%, suggesting no significant off-target effects among those evaluated in the panel (Supplemental Table 1).

Discussion

EPO has emerged as a pleiotropic cytokine that is important not only in the regulation of erythroid cell differentiation and survival but also as a potent cytoprotective agent in multiple organs. The characterization of the tissue-protective effects of EPO has led to the identification of two distinct receptors for EPO: an EPOR/EPOR homodimer that mediates erythropoiesis and an EPOR/CD131 heteromeric receptor that mediates tissue-protective effects. Here we describe the discovery and characterization of the nonpeptidyl compound STS-E412, which selectively activates the tissue-protective EPOR/CD131 receptor.

The first reports of nonpeptidyl small molecule EPO receptor agonists described compounds activating the EPOR/EPOR homodimer. These compounds demonstrated EPO-like activities on hematopoietic precursor cells in vitro, while the potencies were relatively low ($EC_{50} > 1$ μM), and the compounds had molecular masses >1000 Da (Qureshi et al., 1999; Goldberg et al., 2002). A dimeric 21-amino-acid peptide lacking sequence homology with EPO also activated the EPOR/EPOR homodimer in preclinical and clinical studies (Wrighton et al., 1996; Johnson et al., 1998; Besarab et al., 2012). The crystal structure of the dimeric EPO mimetic

peptide bound to the EPOR confirmed that the binding is orthosteric (Livnah et al., 1996). Although none of these mimetics are likely to be orally bioavailable, these studies demonstrated the feasibility of developing small molecules that compete with EPO to bind the EPOR/EPOR homodimer.

Given the similarities in the mechanisms of activation and structures of the receptors for TPO and EPO (Vigon et al., 1992; Boulay et al., 2003), the success in discovering and developing small molecule TPOR agonists has further suggested the feasibility of discovering small molecule mimetics of EPO. All the small molecule TPOR agonists reported to date activate the receptor by binding to allosteric sites outside of the native ligand-binding site and proximal to residues near the plasma membrane (Desjardins et al., 2006; Dziewanowska et al., 2007; Kim et al., 2007; Erickson-Miller et al., 2009; Kalota and Gewirtz, 2010; Abe et al., 2011), suggesting that allosteric compounds may have more promise as therapeutic agents targeting the EPO receptor when compared with compounds binding at the orthosteric sites. The allosteric TPOR agonists described to date are also smaller than the previously described orthosteric EPOR agonists, supporting the potential to design compounds that cross the BBB. Allosteric small peptide agonists of the EPO receptor have been described, but no tissue-protective effects were reported (Naranda et al., 1999, 2002). Small molecule compounds selective for the tissue-protective EPOR/CD131 heterodimer have the potential to overcome the limitations of EPO regarding tissue availability and may improve safety by avoiding the hematopoietic side effects.

A fundamental mechanism of the EPO-induced protective effect is the inhibition of apoptosis via the JAK2/AKT pathway and subsequent transcriptional regulation of anti-apoptotic proteins, including Bcl-xL and Bax (Digicaylioglu and Lipton, 2001; Wen et al., 2002; Um and Lodish, 2006; Wu et al., 2007a). EPO also protects cells against oxidative damage in vitro and in vivo (Solaroglu et al., 2003; Wu et al., 2007b). STS-E412 activates the tissue protective EPOR/CD131 receptor at nanomolar concentrations in primary human neuronal cells and cell lines stably expressing the EPOR and CD131. The magnitude of CD131 phosphorylation in response to STS-E412 was comparable to that induced by rhEPO in EPOR/CD131 transfectants. STS-E412 also increased phosphorylation of EPOR in these transfectants, but the magnitude of the effect was substantially lower than that induced by rhEPO. STS-E412 triggered JAK2 and AKT phosphorylation in the EPOR/CD131 transfectants with a maximal increase approximately 50% of that induced by rhEPO. No significant activation of the EPOR/EPOR homodimer by STS-E412 was observed, illustrating selective activation of the EPOR/CD131 receptor by STS-E412. In contrast to transfected cell lines, the maximal effects of STS-E412 in primary neuronal cells were comparable to rhEPO regarding both EPOR phosphorylation and cytoprotection. The lack of EPOR phosphorylation in transfectants expressing the EPOR alone and the absence of EPO-like proliferative effects in TF-1 and primary human $CD34^+$ hematopoietic progenitor cells further support the view that STS-E412 does not effectively activate EPOR/EPOR homodimeric receptors. The difference in the relative effects of rhEPO and STS-E412 on the EPOR/CD131 transfectants and primary cells is likely due to the presence of both EPOR/EPOR and EPOR/CD131 receptors in the heterologous expression system, while primary human neuronal cells express primarily the EPOR/CD131 receptor (Brines et al., 2004). Previous studies demonstrating comparable cytoprotective effects of CEPO and EPO in nonhematopoietic tissues, including the CNS and kidneys (Leist et al., 2004; Imamura et al., 2007; Wang et al., 2007), also support the conclusion that the primary receptor for EPO on neurons and RPTEC is EPOR/CD131.

Proliferation assays in TF-1 and $CD34^+$ progenitor cells provide a more complex view of interactions between STS-E412 and cell surface receptors. TF-1 cells express IL-3, IL-5, and GM-CSF receptors (heteromeric receptors composed of distinct α subunits and CD131), and these cytokines stimulate TF-1 cell proliferation. TF-1 cells also express TPOR and thrombopoietin stimulates TF-1 cell proliferation (Drexler and Quentmeier, 1996). That STS-E412 does not stimulate proliferation in TF-1 cells suggests that STS-E412 does not effectively interact with these receptors at concentrations below 3–10 μM. The observed decrease in TF-1 proliferation at higher concentrations may suggest STS-E412–mediated sequestration of the CD131 subunit, which is required for growth of the IL-3– or GM-CSF–dependent TF-1 cells. In contrast to TF-1 cells, the increase in $CD34^+$ progenitor cell proliferation at STS-E412 concentrations above 3–10 μM may suggest a low-affinity interaction with the EPOR/EPOR homodimer or TPOR, although this was not detectable in the receptor phosphorylation assays. The increase in $CD34^+$ cell proliferation also suggests that the decrease in TF-1 proliferation at high concentrations is not due to a nonspecific cytotoxic effect of STS-E412. Regardless of the mechanism underlying these contrasting results with different cell types, these effects occurred at STS-E412 concentrations several orders-of-magnitude above those producing cytoprotective effects and EPOR/CD131 receptor activation.

STS-E412 exhibited a bell-shaped dose-response curve in the EPOR/CD131 transfectants and RPTEC cells, but not in primary neuronal cells. These observations are not surprising in light of previous studies on the small molecule TPOR agonist eltrombopag, which resulted in bell-shaped dose-response curves in receptor-expressing cell lines (Xie et al., 2012). In addition, eltrombopag triggered TPO-like STAT5 activation in $CD34^+CD41^-$ progenitor cells, but in contrast to rhTPO, eltrombopag did not activate STAT3 or AKT in $CD34^+CD41^+$ cells (Sun et al., 2012). Bell-shaped dose-response curves were also observed in previous in vitro studies on nonpeptidyl compounds activating the receptors for G-CSF and EPO (Tian et al., 1998; Qureshi et al., 1999). The formation of 1:1 receptor/ligand complex at high ligand concentrations was also shown to inhibit the activation of receptors for growth hormone and EPO (Fuh et al., 1992; Schneider et al., 1997). The crystal structure of the GM-CSF receptor in complex with CD131 revealed a 2:2:2 hexamer consisting of two GM-CSFR α chains, two CD131 chains, and two GM-CSF molecules, and also demonstrated the existence of a functional higher-order dodecamer, a hexamer dimer (Hansen et al., 2008). The higher-order structures of the EPOR/CD131 complex are not known, but the GM-CSFRα/CD131 data suggest that similar higher-order structures form when CD131 associates with the EPOR. The bell-shaped dose-response curve triggered by STS-E412 suggests that, similar to the EPOR/EPOR, growth hormone, G-CSF, and GM-CSF receptors, the formation of 1:1 receptor/ligand complex at high STS-E412 concentrations prevents the optimal activation of

the EPOR/CD131 receptor. However, the exact mechanism of receptor activation by STS-E412 remains to be elucidated.

In the primary neuronal and kidney cell cytoprotection assays, STS-E412 exhibited significant cytoprotective effects after a range of cytotoxic challenges. These data are consistent with previous reports demonstrating broad cytoprotective effects of rhEPO, EPO variants selective for EPOR/CD131, and mimetic peptides (Konishi et al., 1993; Sakanaka et al., 1998; Erbayraktar et al., 2003; Brines et al., 2004, 2008; Leist et al., 2004; Coleman et al., 2006, Ahmet et al., 2011; Chen et al., 2012). The maximal protective effects in response to STS-E412 were comparable to those induced by rhEPO, and optimal responses were observed at low nanomolar concentrations in both neurons and RPTEC. It is worth noting that staurosporine inhibits many intracellular kinases and may inhibit activation of the tissue-protective EPOR/CD131 receptor and signaling molecules involved in protection. Our experimental paradigm used a 24-hour pretreatment (in the absence of staurosporine) and staurosporine concentrations used in our experiments were relatively low, but we cannot exclude the possibility that kinase inhibition affected the observed cytoprotective effects of rhEPO and STS-E412. This concern, however, does not associate with cytoprotective effects observed after glutamate and H_2O_2 challenge.

In summary, we report the discovery of STS-E412, which selectively activates the tissue-protective EPOR/CD131 heteromeric receptor. The small size, permeability across PAMPA and Caco-2 cellular monolayers, and observed CNS availability in vivo suggest improved tissue permeability compared with previously described nonpeptidyl EPO receptor agonists. Combined with the EPO-like protective effects in primary neurons and RPTEC, these compound characteristics support further evaluation of STS-E412 in neurodegenerative diseases and organ protection.

Authorship Contributions

Participated in research design: Miller, Church, Leonoudakis, Lariosa-Willingham, Frigon, Tettenborn, Spencer, Punnonen.

Conducted experiments: Miller, Church, Leonoudakis, Lariosa-Willingham, Frigon, Tettenborn, Spencer, Punnonen.

Contributed new reagents or analytic tools: Miller, Church, Tettenborn, Spencer, Punnonen.

Wrote or contributed to the writing of the manuscript: Miller, Church, Leonoudakis, Lariosa-Willingham, Frigon, Tettenborn, Spencer, Punnonen.

References

Abe M, Suzuki K, Sakata C, Sugasawa K, Hirayama F, Koga Y, Kawasaki T, Naganuma S, and Itoh H (2011) Pharmacological profile of AS1670542, a novel orally-active human thrombopoietin receptor agonist. *Eur J Pharmacol* **650**:58–63.

Ahmet I, Tae HJ, Juhaszova M, Riordon DR, Boheler KR, Sollott SJ, Brines M, Cerami A, Lakatta EG, and Talan MI (2011) A small nonerythropoietic helix B surface peptide based upon erythropoietin structure is cardioprotective against ischemic myocardial damage. *Mol Med* **17**:194–200.

Assaraf MI, Diaz Z, Liberman A, Miller WHJ, Jr, Arvanitakis Z, Li Y, Bennett DA, and Schipper HM (2007) Brain erythropoietin receptor expression in Alzheimer disease and mild cognitive impairment. *J Neuropathol Exp Neurol* **66**:389–398.

Bennis Y, Sarlon-Bartoli G, Guillet B, Lucas L, Pellegrini L, Velly L, Blot-Chabaud M, Dignat-Georges F, Sabatier F, and Pisano P (2012) Priming of late endothelial progenitor cells with erythropoietin before transplantation requires the CD131 receptor subunit and enhances their angiogenic potential. *J Thromb Haemost* **10**: 1914–1928.

Besarab A, Zeig SN, Martin ER, Pergola PE, Whittier FC, Zabaneh RI, Schiller B, Mayo M, Francisco CA, and Polu KR et al. (2012) An open-label, sequential, dose-finding study of peginesatide for the maintenance treatment of anemia in chronic hemodialysis patients. *BMC Nephrol* **13**:95.

Boulay JL, O'Shea JJ, and Paul WE (2003) Molecular phylogeny within type I cytokines and their cognate receptors. *Immunity* **19**:159–163.

Brines M and Cerami A (2008) Erythropoietin-mediated tissue protection: reducing collateral damage from the primary injury response. *J Intern Med* **264**: 405–432.

Brines M, Grasso G, Fiordaliso F, Sfacteria A, Ghezzi P, Fratelli M, Latini R, Xie QW, Smart J, and Su-Rick CJ et al. (2004) Erythropoietin mediates tissue protection through an erythropoietin and common beta-subunit heteroreceptor. *Proc Natl Acad Sci USA* **101**:14907–14912.

Brines M, Patel NS, Villa P, Brines C, Mennini T, De Paola M, Erbayraktar Z, Erbayraktar S, Sepodes B, and Thiemermann C et al. (2008) Nonerythropoietic, tissue-protective peptides derived from the tertiary structure of erythropoietin. *Proc Natl Acad Sci USA* **105**:10925–10930.

Brines ML, Ghezzi P, Keenan S, Agnello D, de Lanerolle NC, Cerami C, Itri LM, and Cerami A (2000) Erythropoietin crosses the blood-brain barrier to protect against experimental brain injury. *Proc Natl Acad Sci USA* **97**:10526–10531.

Calvillo L, Latini R, Kajstura J, Leri A, Anversa P, Ghezzi P, Salio M, Cerami A, and Brines M (2003) Recombinant human erythropoietin protects the myocardium from ischemia-reperfusion injury and promotes beneficial remodeling. *Proc Natl Acad Sci USA* **100**:4802–4806.

Carr PD, Gustin SE, Church AP, Murphy JM, Ford SC, Mann DA, Woltring DM, Walker I, Ollis DL, and Young IG (2001) Structure of the complete extracellular domain of the common beta subunit of the human GM-CSF, IL-3, and IL-5 receptors reveals a novel dimer configuration. *Cell* **104**:291–300.

Chateauvieux S, Grigorakaki C, Morceau F, Dicato M, and Diederich M (2011) Erythropoietin, erythropoiesis and beyond. *Biochem Pharmacol* **82**:1291–1303.

Chen H, Spagnoli F, Burris M, Rolland WB, Fajilan A, Dou H, Tang J, and Zhang JH (2012) Nanoerythropoietin is 10-times more effective than regular erythropoietin in neuroprotection in a neonatal rat model of hypoxia and ischemia. *Stroke* **43**: 884–887.

Coleman TR, Westenfelder C, Tögel FE, Yang Y, Hu Z, Swenson L, Leuvenink HG, Ploeg RJ, d'Uscio LV, and Katusic ZS et al. (2006) Cytoprotective doses of erythropoietin or carbamylated erythropoietin have markedly different procoagulant and vasoactive activities. *Proc Natl Acad Sci USA* **103**:5965–5970.

David RB, Lim GB, Moritz KM, Koukoulas I, and Wintour EM (2002) Quantitation of the mRNA levels of Epo and EpoR in various tissues in the ovine fetus. *Mol Cell Endocrinol* **188**:207–218.

Desjardins RE, Tempel DL, Lucek R, and Kuter DJ (2006) Single and multiple oral doses of AKR-501 (YM477) increase the platelet count in healthy volunteers (abstract). *Blood* **108**(Suppl):abstract 477.

Digicaylioglu M and Lipton SA (2001) Erythropoietin-mediated neuroprotection involves cross-talk between Jak2 and NF-κB signalling cascades. *Nature* **412**: 641–647.

Drexler HG and Quentmeier H (1996) Thrombopoietin: expression of its receptor MPL and proliferative effects on leukemic cells. *Leukemia* **10**:1405–1421.

Drüeke TB, Locatelli F, Clyne N, Eckardt KU, Macdougall IC, Tsakiris D, Burger HU, and Scherhag A; CREATE Investigators (2006) Normalization of hemoglobin level in patients with chronic kidney disease and anemia. *N Engl J Med* **355**: 2071–2084.

Dziewanowska ZE, Matsumoto RM, Zhang JK, Schindler K, Loewen G, Doherty JP, Berg JK, and Newberry B (2007) Single and multiple oral doses of LGD-4665, a small molecule thrombopoietin receptor agonist, increase platelet counts in healthy male subjects (abstract). *Blood* **110**(Suppl):abstract 1298.

Eckardt KU and Kurtz A (2005) Regulation of erythropoietin production. *Eur J Clin Invest* **35** (Suppl 3):13–19.

Ehrenreich H, Kästner A, Weissenborn K, Streeter J, Sperling S, Wang KK, Worthmann H, Hayes RL, von Ahsen N, and Kastrup A et al. (2011) Circulating damage marker profiles support a neuroprotective effect of erythropoietin in ischemic stroke patients. *Mol Med* **17**:1306–1310.

Erbayraktar S, Grasso G, Sfacteria A, Xie QW, Coleman T, Kreilgaard M, Torup L, Sager T, Erbayraktar Z, and Gokmen N et al. (2003) Asialoerythropoietin is a nonerythropoietic cytokine with broad neuroprotective activity in vivo. *Proc Natl Acad Sci USA* **100**:6741–6746.

Erickson-Miller CL, Delorme E, Tian SS, Hopson CB, Landis AJ, Valoret EI, Sellers TS, Rosen J, Miller SG, and Luengo JI et al. (2009) Preclinical activity of eltrombopag (SB-497115), an oral, nonpeptide thrombopoietin receptor agonist. *Stem Cells* **27**:424–430.

Erickson-Miller CL, DeLorme E, Tian SS, Hopson CB, Stark K, Giampa L, Valoret EI, Duffy KJ, Luengo JL, and Rosen J et al. (2005) Discovery and characterization of a selective, nonpeptidyl thrombopoietin receptor agonist. *Exp Hematol* **33**:85–93.

Fuh G, Cunningham BC, Fukunaga R, Nagata S, Goeddel DV, and Wells JA (1992) Rational design of potent antagonists to the human growth hormone receptor. *Science* **256**:1677–1680.

Goldberg J, Jin Q, Ambroise Y, Satoh S, Desharnais J, Capps K, and Boger DL (2002) Erythropoietin mimetics derived from solution phase combinatorial libraries. *J Am Chem Soc* **124**:544–555.

Grasso G, Sfacteria A, Passalacqua M, Morabito A, Buemi M, Macrì B, Brines ML, and Tomasello F (2005) Erythropoietin and erythropoietin receptor expression after experimental spinal cord injury encourages therapy by exogenous erythropoietin. *Neurosurgery* **56**:821–827, discussion 821–827.

Hanazono Y, Sasaki K, Nitta H, Yazaki Y, and Hirai H (1995) Erythropoietin induces tyrosine phosphorylation of the beta chain of the GM-CSF receptor. *Biochem Biophys Res Commun* **208**:1060–1066.

Hansen G, Hercus TR, McClure BJ, Stomski FC, Dottore M, Powell J, Ramshaw H, Woodcock JM, Xu Y, and Guthridge M et al. (2008) The structure of the GM-CSF receptor complex reveals a distinct mode of cytokine receptor activation. *Cell* **134**: 496–507.

Hitchcock SA (2008) Blood-brain barrier permeability considerations for CNS-targeted compound library design. *Curr Opin Chem Biol* **12**:318–323.

Imamura R, Isaka Y, Ichimaru N, Takahara S, and Okuyama A (2007) Carbamylated erythropoietin protects the kidneys from ischemia-reperfusion injury without stimulating erythropoiesis. *Biochem Biophys Res Commun* **353**:786–792.

Jacobson LO, Goldwasser E, Fried W, and Plzak LF (1957) Studies on erythropoiesis. VII. The role of the kidney in the production of erythropoietin. *Trans Assoc Am Physicians* **70**:305–317.

Jang W, Park J, Shin KJ, Kim JS, Kim JS, Youn J, Cho JW, Oh E, Ahn JY, and Oh KW et al. (2014) Safety and efficacy of recombinant human erythropoietin treatment of non-motor symptoms in Parkinson's disease. *J Neurol Sci* **337**: 47–54.

Johnson DL, Farrell FX, Barbone FP, McMahon FJ, Tullai J, Hoey K, Livnah O, Wrighton NC, Middleton SA, and Loughney DA et al. (1998) Identification of a 13 amino acid peptide mimetic of erythropoietin and description of amino acids critical for the mimetic activity of EMP1. *Biochemistry* **37**:3699–3710.

Joshi D, Abraham D, Shiwen X, Baker D, and Tsui J (2014) Potential role of erythropoietin receptors and ligands in attenuating apoptosis and inflammation in critical limb ischemia. *J Vasc Surg* **60**:191–201, e1–e2.

Jubinsky PT, Krijanovski OI, Nathan DG, Tavernier J, and Sieff CA (1997) The beta chain of the interleukin-3 receptor functionally associates with the erythropoietin receptor. *Blood* **90**:1867–1873.

Juul SE, Anderson DK, Li Y, and Christensen RD (1998) Erythropoietin and erythropoietin receptor in the developing human central nervous system. *Pediatr Res* **43**: 40–49.

Kalota A and Gewirtz AM (2010) A prototype nonpeptidyl, hydrazone class, thrombopoietin receptor agonist, SB-559457, is toxic to primary human myeloid leukemia cells. *Blood* **115**:89–93.

Kim MJ, Park SH, Opella SJ, Marsilje TH, Michellys PY, Seidel HM, and Tian SS (2007) NMR structural studies of interactions of a small, nonpeptidyl Tpo mimic with the thrombopoietin receptor extracellular juxtamembrane and transmembrane domains. *J Biol Chem* **282**:14253–14261.

Konishi Y, Chui DH, Hirose H, Kunishita T, and Tabira T (1993) Trophic effect of erythropoietin and other hematopoietic factors on central cholinergic neurons in vitro and in vivo. *Brain Res* **609**:29–35.

Kunioku H, Inoue K, and Tomida M (2001) Interleukin-6 protects rat PC12 cells from serum deprivation or chemotherapeutic agents through the phosphatidylinositol 3-kinase and STAT3 pathways. *Neurosci Lett* **309**:13–16.

Kuter DJ (2013) The biology of thrombopoietin and thrombopoietin receptor agonists. *Int J Hematol* **98**:10–23.

Leist M, Ghezzi P, Grasso G, Bianchi R, Villa P, Fratelli M, Savino C, Bianchi M, Nielsen J, and Gerwien J et al. (2004) Derivatives of erythropoietin that are tissue protective but not erythropoietic. *Science* **305**:239–242.

Liu C, Shen K, Liu Z, and Noguchi CT (1997) Regulated human erythropoietin receptor expression in mouse brain. *J Biol Chem* **272**:32395–32400.

Livnah O, Stura EA, Johnson DL, Middleton SA, Mulcahy LS, Wrighton NC, Dower WJ, Jolliffe LK, and Wilson IA (1996) Functional mimicry of a protein hormone by a peptide agonist: the EPO receptor complex at 2.8 A. *Science* **273**:464–471.

Livnah O, Stura EA, Middleton SA, Johnson DL, Jolliffe LK, and Wilson IA (1999) Crystallographic evidence for preformed dimers of erythropoietin receptor before ligand activation. *Science* **283**:987–990.

Mammis A, McIntosh TK, and Maniker AH (2009) Erythropoietin as a neuroprotective agent in traumatic brain injury Review. *Surg Neurol* **71**:527–531, discussion 531.

Medana IM, Day NP, Hien TT, White NJ, and Turner GD (2009) Erythropoietin and its receptors in the brainstem of adults with fatal falciparum malaria. *Malar J* **8**: 261.

Nachbauer W, Hering S, Seifert M, Steinkellner H, Sturm B, Scheiber-Mojdehkar B, Reindl M, Strasak A, Poewe W, and Weiss G et al. (2011) Effects of erythropoietin on frataxin levels and mitochondrial function in Friedreich ataxia—a dose-response trial. *Cerebellum* **10**:763–769.

Naranda T, Kaufman RI, Li J, Wong K, Boge A, Hallén D, Fung KY, Duncan MW, Andersen N, and Goldstein A et al. (2002) Activation of erythropoietin receptor through a novel extracellular binding site. *Endocrinology* **143**:2293–2302.

Naranda T, Wong K, Kaufman RI, Goldstein A, and Olsson L (1999) Activation of erythropoietin receptor in the absence of hormone by a peptide that binds to a domain different from the hormone binding site. *Proc Natl Acad Sci USA* **96**: 7569–7574.

Punnonen J, Tettenborn C, Church T, Muench M, Collier T, and Spencer J. (2011) A nonpeptidic erythropoietin mimetic STS-E15 protects primary neurons against 6-hydroxydopamine or glutamate toxicity without erythropoietic activity, in *Proceedings of the 63rd Annual Meeting of the American Academy of Neurology;* 2011 Apr 9–16; Honolulu, HI. Abstract 335AAN11D1, American Academy of Neurology, Minneapolis, MN.

Punnonen J, Miller J, Collier T, and Spencer J (2015) Agonists of the Tissue-Protective Erythropoietin Receptor in the Treatment of Parkinson's Disease. *Current Topics in Med Chem* **15**:955–969.

Puskovic V, Wolfe D, Wechuck J, Krisky D, Collins J, Glorioso JC, Fink DJ, and Mata M (2006) HSV-mediated delivery of erythropoietin restores dopaminergic function in MPTP-treated mice. *Mol Ther* **14**:710–715.

Qureshi SA, Kim RM, Konteatis Z, Biazzo DE, Motamedi H, Rodrigues R, Boice JA, Calaycay JR, Bednarek MA, and Griffin P et al. (1999) Mimicry of erythropoietin by a nonpeptide molecule. *Proc Natl Acad Sci USA* **96**:12156–12161.

Sakanaka M, Wen TC, Matsuda S, Masuda S, Morishita E, Nagao M, and Sasaki R (1998) In vivo evidence that erythropoietin protects neurons from ischemic damage. *Proc Natl Acad Sci USA* **95**:4635–4640.

Savino C, Pedotti R, Baggi F, Ubiali F, Gallo B, Nava S, Bigini P, Barbera S, Fumagalli E, and Mennini T et al. (2006) Delayed administration of erythropoietin and its non-erythropoietic derivatives ameliorates chronic murine autoimmune encephalomyelitis. *J Neuroimmunol* **172**:27–37.

Schneider H, Chaovapong W, Matthews DJ, Karkaria C, Cass RT, Zhan H, Boyle M, Lorenzini T, Elliott SG, and Giebel LB (1997) Homodimerization of erythropoietin receptor by a bivalent monoclonal antibody triggers cell proliferation and differentiation of erythroid precursors. *Blood* **89**:473–482.

Singh AK, Szczech L, Tang KL, Barnhart H, Sapp S, Wolfson M, and Reddan D; CHOIR Investigators (2006) Correction of anemia with epoetin alfa in chronic kidney disease. *N Engl J Med* **355**:2085–2098.

Solaroglu I, Solaroglu A, Kaptanoglu E, Dede S, Haberal A, Beskonakli E, and Kilinc K (2003) Erythropoietin prevents ischemia-reperfusion from inducing oxidative damage in fetal rat brain. *Childs Nerv Syst* **19**:19–22.

Su KH, Shyue SK, Kou YR, Ching LC, Chiang AN, Yu YB, Chen CY, Pan CC, and Lee TS (2011) β Common receptor integrates the erythropoietin signaling in activation of endothelial nitric oxide synthase. *J Cell Physiol* **226**:3330–3339.

Sun H, Tsai Y, Nowak I, Liesveld J, and Chen Y (2012) Eltrombopag, a thrombopoietin receptor agonist, enhances human umbilical cord blood hematopoietic stem/primitive progenitor cell expansion and promotes multi-lineage hematopoiesis. *Stem Cell Res (Amst)* **9**:77–86.

Tian SS, Lamb P, King AG, Miller SG, Kessler L, Luengo JI, Averill L, Johnson RK, Gleason JG, and Pelus LM et al. (1998) A small, nonpeptidyl mimic of granulocyte-colony-stimulating factor. *Science* **281**:257–259.

Um M and Lodish HF (2006) Antiapoptotic effects of erythropoietin in differentiated neuroblastoma SH-SY5Y cells require activation of both the STAT5 and AKT signaling pathways. *J Biol Chem* **281**:5648–5656.

Vigon I, Mornon JP, Cocault L, Mitjavila MT, Tambourin P, Gisselbrecht S, and Souyri M (1992) Molecular cloning and characterization of MPL, the human homolog of the v-mpl oncogene: identification of a member of the hematopoietic growth factor receptor superfamily. *Proc Natl Acad Sci USA* **89**:5640–5644.

Wager TT, Hou X, Verhoest PR, and Villalobos A (2010) Moving beyond rules: the development of a central nervous system multiparameter optimization (CNS MPO) approach to enable alignment of druglike properties. *ACS Chem Neurosci* **1**:435–449.

Wang Y, Zhang ZG, Rhodes K, Renzi M, Zhang RL, Kapke A, Lu M, Pool C, Heavner G, and Chopp M (2007) Post-ischemic treatment with erythropoietin or carbamylated erythropoietin reduces infarction and improves neurological outcome in a rat model of focal cerebral ischemia. *Br J Pharmacol* **151**:1377–1384.

Wen TC, Sadamoto Y, Tanaka J, Zhu PX, Nakata K, Ma YJ, Hata R, and Sakanaka M (2002) Erythropoietin protects neurons against chemical hypoxia and cerebral ischemic injury by up-regulating Bcl-xL expression. *J Neurosci Res* **67**:795–803.

Wogulis M, Wright S, Cunningham D, Chilcote T, Powell K, and Rydel RE (2005) Nucleation-dependent polymerization is an essential component of amyloid-mediated neuronal cell death. *J Neurosci* **25**:1071–1080.

Wrighton NC, Farrell FX, Chang R, Kashyap AK, Barbone FP, Mulcahy LS, Johnson DL, Barrett RW, Jolliffe LK, and Dower WJ (1996) Small peptides as potent mimetics of the protein hormone erythropoietin. *Science* **273**:458–464.

Wu Y, Shang Y, Sun S, Liang H, and Liu R (2007a) Erythropoietin prevents PC12 cells from 1-methyl-4-phenylpyridinium ion-induced apoptosis via the Akt/GSK-3beta/caspase-3 mediated signaling pathway. *Apoptosis* **12**:1365–1375.

Wu Y, Shang Y, Sun S, and Liu R (2007b) Antioxidant effect of erythropoietin on 1-methyl-4-phenylpyridinium-induced neurotoxicity in PC12 cells. *Eur J Pharmacol* **564**:47–56.

Xie C-Y, Xu Y-P, Zhao H-B, and Lou L-G (2012) A novel and simple hollow-fiber assay for *in vivo* evaluation of nonpeptidyl thrombopoietin receptor agonists. *Exp Hematol* **40**:386–392.

Address correspondence to: Dr. James L. Miller, STATegics, Inc, 1455 Adams Drive, Menlo Park, CA 94025. E-mail: jim.miller@stategics.com